Available online at www.sciencedirect.com

SCIENCE DIRECT®

Developmental Biology 272 (2004) 231–247

DEVELOPMENTAL BIOLOGY

www.elsevier.com/locate/ydbio

Structure–function analysis of the *Drosophila* retinal determination protein Dachshund

Beril C. Tavsanli,[a] Edwin J. Ostrin,[b] Heather K. Burgess,[c] Brooke W. Middlebrooks,[c] Tuan A. Pham,[c] and Graeme Mardon[a,b,c,d,e,*]

[a] *Program in Developmental Biology, Baylor College of Medicine, Houston, TX 77030, USA*
[b] *Department of Molecular and Human Genetics, Baylor College of Medicine, Houston, TX 77030, USA*
[c] *Department of Pathology, Baylor College of Medicine, Houston, TX 77030, USA*
[d] *Department of Neuroscience, Baylor College of Medicine, Houston, TX 77030, USA*
[e] *Department of Ophthalmology, Baylor College of Medicine, Houston, TX 77030, USA*

Received for publication 18 March 2004, accepted 4 May 2004

Abstract

Dachshund (Dac) is a highly conserved nuclear protein that is distantly related to the Ski/Sno family of corepressor proteins. In *Drosophila*, Dac is necessary and sufficient for eye development and, along with Eyeless (Ey), Sine oculis (So), and Eyes absent (Eya), forms the core of the retinal determination (RD) network. In vivo and in vitro experiments suggest that members of the RD network function together in one or more complexes to regulate the expression of downstream targets. For example, Dac and Eya synergize in vivo to induce ectopic eye formation and they physically interact through conserved domains. Dac contains two highly conserved domains, named DD1 and DD2, but no function has been assigned to either of them in an in vivo context. We performed structure–function studies to understand the relationship between the conserved domains of Dac and the rest of the protein and to determine the function of each domain during development. We show that only DD1 is essential for Dac function and while DD2 facilitates DD1, it is not absolutely essential in spite of more than 500 million years of conservation. Moreover, the physical interaction between Eya and DD2 is not required for the genetic synergy between the two proteins. Finally, we show that DD1 also plays a central role for nuclear localization of Dac.

Keywords: Dachshund; *dac*; Eye; Leg; Mushroom body; *Drosophila*; Structure–function

Introduction

Tissue-specific nuclear factors play important roles during cell fate determination. These factors can work in multiple combinations to regulate the development of different tissues. Dachshund (Dac) is one such factor that is required for the normal development of diverse organs such as the eye, antenna, brain, leg, and genitals (Dong et al., 2002; Keisman and Baker, 2001; Kurusu et al., 2000; Mardon et al., 1994; Martini et al., 2000; Noveen et al., 2000). During *Drosophila* eye development, Dac collaborates with three other nuclear factors, Eyeless (Ey), Sine oculis (So), and Eyes absent (Eya), to determine retinal cell fates, forming the core of the so-called retinal determination (RD) network (Chen et al., 1999). RD network genes are necessary and sufficient to initiate eye development since eye-specific mutations in each gene result in eyeless animals and ectopic expression of each (except *so*) is sufficient to induce ectopic eyes (Bonini et al., 1993, 1997; Chen et al., 1997; Cheyette et al., 1994; Halder et al., 1995, 1998; Mardon et al., 1994; Quiring et al., 1994; Shen and Mardon, 1997). RD genes are thought to function in an interdependent network instead of a linear hierarchy since misexpression of any one gene (except *so*) is sufficient to induce expression of all others and ectopic eye induction does not occur in animals missing any one of these genes (Bonini et al., 1997; Chen et al., 1997; Halder et al., 1998; Shen and Mardon, 1997). In addition, co-misexpression of members of the RD network acts synergistically to induce larger eyes with higher penetrance in a variety of tissues (Bonini et al., 1997; Chen et al., 1997; Pignoni et al., 1997). For example,

* Corresponding author. Department of Pathology, Baylor College of Medicine, One Baylor Plaza, Room T222, Houston, TX 77030. Fax: +1-713-798-3359.
E-mail address: gmardon@bcm.tmc.edu (G. Mardon).

0012-1606/$ - see front matter © 2004 Elsevier Inc. All rights reserved.
doi:10.1016/j.ydbio.2004.05.005

ectopic eyes induced by Eya or Dac alone are limited to the antenna whereas misexpressing both results in ectopic eye induction on the legs and thorax as well (Chen et al., 1997).

All RD proteins have highly conserved homologs in other organisms ranging from *C. elegans* to humans. Dac has two homologs in humans and mice, termed DACH1/2 and Dach1/2, respectively. Dach1 and Dach2 expression patterns overlap extensively in the eye, limbs, and brain (Caubit et al., 1999; Davis et al., 1999, 2001b; Hammond et al., 1998). Dach1 knockout mice die postnatally without any gross morphological abnormalities in these tissues, suggesting that Dach1 and Dach2 may function redundantly (Backman et al., 2003; Davis et al., 2001a). The region of homology between Dac (a 1081 amino acid protein) and its mammalian counterparts is limited to three specific domains (Fig. 1). First, a polyglutamine stretch is present near the N-terminus of *Drosophila* Dac while a polyserine run is present in DACH1. However, both domains are encoded by a CAG repeat. Second, the most highly conserved domain of Dac, termed DD1 (Dac domain 1), is 107 amino acids (aa) in length and is 78% identical (86% similar) to human DACH1. Finally, a third conserved domain of Dac, termed DD2 (Dac domain 2), is 81 aa long and is 58% identical (73% similar) to human DACH1 (Davis et al., 1999; Hammond et al., 1998). Ey contains a paired domain and a homeodomain, two highly conserved

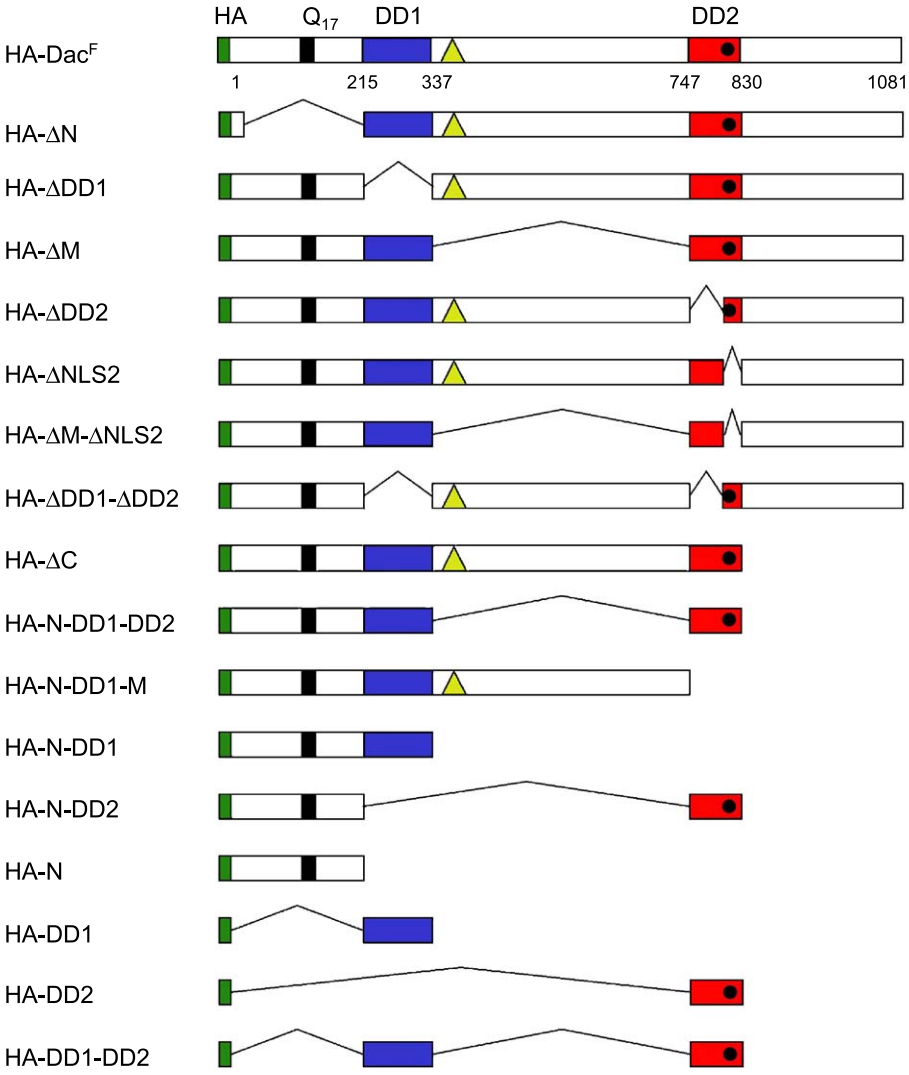

Fig. 1. Schematic of *UAS-HA-dac* rescue constructs. The black box denotes a 17 amino acid (aa) long polyglutamine (Q_{17}) stretch. Dachshund Domain 1 (DD1) includes aa 215–337 and is indicated in blue. Since the cDNA we used includes a short exon that can be alternatively spliced and is not conserved in humans, the DD1 used in these constructs is 123 aa long instead of 107 aa. Dachshund Domain 2 (DD2) includes aa 747–830 and is indicated in red. All constructs encode an amino-terminal HA-tag for specific detection (green box). PSORTII motif prediction software detects two putative NLS sequences in Dac: NLS1, denoted by the yellow triangle, includes aa 353–359; and NLS2, denoted by the black circle, includes aa 803–819. Internal deletions in each protein are denoted by thin connector lines. Since NLS2 could have been essential for nuclear transport of Dac, we kept NLS2 in ΔDD2 and deleted it in a separate construct (ΔNLS2). Multiple transgenic lines were obtained and tested for each construct. To perform the rescue assay, all UAS transgenes were driven by dac^{GAL4} in a *dac* null background. Dac^{F} = full-length Dac; N = N-terminal domain; M = middle domain; C = C-terminal domain; HA = 11 aa long hemagglutin tag fused at the N-terminus.

DNA binding domains, and is a homolog of vertebrate Pax6. So contains a homeodomain and a novel domain (the Six domain) named for its conservation in the vertebrate Six family of proteins. Eya has a C-terminal conserved domain (ECD-1), which recently has been shown to function as a tyrosine phosphatase of the haloacid dehalogenase superfamily (Li et al., 2003; Rayapureddi et al., 2003; Tootle et al., 2003). In addition, Eya has a proline/serine/threonine-rich PST domain with transactivation function, a smaller conserved ECD-2 domain, and two conserved MAPK phosphorylation sites (Hsiao et al., 2001; Silver et al., 2003). For a review of mammalian homologs of the RD genes, see Hanson (2001).

Evolutionary conservation can be accounted for by a functional constraint on amino acid substitution. Therefore, stretches of amino acid sequences (domains) conserved across phylogeny are likely to represent functionally important regions in a protein. Several lines of evidence suggest that conserved domains perform the most critical functions of Dac. First, when expressed in *Drosophila*, chick *Dach2* can rescue the no-eye phenotype of *dac* mutant flies, even though these proteins are highly divergent outside of the conserved domains DD1 and DD2 (Heanue et al., 1999). Second, yeast two-hybrid and GST pull-down assays suggest that Dac and Eya interact directly through their conserved domains (Chen et al., 1997). Third, similar synergistic and physical interactions between Dac and Eya are preserved in vertebrates. Specifically, a Pax3/Six1/Eya2/Dach2 cassette regulates myogenesis in the chick dermamyotome and all four genes synergize to activate downstream genes such as MyoD and myogenin. In addition, chick Eya2 and Dach2 also directly interact through their conserved domains (Heanue et al., 1999). Similarly, mammalian homologs of RD network proteins act together to regulate myogenesis as well as ear and kidney development in mice (Li et al., 2003). Finally, Dach1 cooperates with Six6 in regulating cell proliferation during mouse retina and pituitary development (Li et al., 2002).

In addition to primary sequence homologies, structural predictions also point to the conserved domains DD1 and DD2 for Dac function. Although not predicted by primary sequence, crystal structure analysis suggests that DD1 from human DACH1 forms a helix-turn-helix motif of the winged helix or forkhead family and is capable of binding DNA (Kim et al., 2002). Furthermore, Dac DD1 shares weak similarity to an N-terminal domain of the Ski/Sno family of proteins and DD2 is structurally similar to a C-terminal domain of Ski/Sno. Both DD2 and the C-terminal domain of Ski are predicted to form an α-helical coiled coil (Davis et al., 1999; Hammond et al., 1998). Ski can homodimerize as well as heterodimerize with Sno through this domain while there is no evidence for homodimerization of Dac (Heyman and Stavnezer, 1994a).

Conservation of domains instead of whole proteins may also suggest modularity of function such that multiple domains may either cooperate toward one function or may each function independently. For example, the paired and homeodomains of Paired are both needed to rescue the *prd* null phenotype, indicating that these two domains are required for *prd* gene function (Bertuccioli et al., 1996). In contrast, the paired and homeodomains of the Ey protein function independently. The paired domain alone is necessary and sufficient for induction of eye development in *Drosophila* while the homeodomain is sufficient to repress other tissue-specific genes such as *distalless* (Punzo et al., 2001). To determine whether the conserved domains of Dac have independent, tissue-specific functions or if they cooperate toward the same function, we conducted a structure–function study. We show that DD1 is the only domain essential for Dac function in all tissues investigated. DD2 increases the efficiency of DD1 function but is dispensable when DD1 is overexpressed. Furthermore, the genetic synergy observed between Eya and Dac does not require the physical interaction between Eya ECD1 and Dac DD2. Finally, since Dac is a nuclear protein, we investigated the mechanism by which it localizes to the nucleus. We find that Dac translocates to the nucleus via a conventional basic nuclear localization signal as well as a novel mechanism involving the conserved domains DD1 and DD2. DD1 plays a central role in nuclear transport since in its absence Dac localization is compromised even with the other domains intact.

Materials and methods

Cloning and fly genetics

An HA epitope tag (MYPYDVPDYA) was subcloned in the *Eco*RI site of pUAST (Brand and Perrimon, 1993) as an adaptor, destroying the 5′ *Eco*RI site to generate the vector pHA. To generate full-length UAS-HA-Dac, a fragment containing the N-terminal 90 bp with a 3′ unique *Sac*II site was PCR amplified from a Dac cDNA clone with the addition of a 5′ *Eco*RI site that allowed in frame fusion of Dac downstream of HA. The PCR product was sequence verified and subcloned into the *Eco*RI–*Sac*II sites of pHA, generating pHA-N1-90. The remaining C-terminal portion of Dac was isolated from a Dac cDNA clone (λ24) that has the E2-E3-E4a splice variant (encoding the longest open reading frame) with a *Sac*II–*Kpn*I digest and subcloned in pHA-N1-90. All manipulations involving deletion of Dac domains were performed in pBluescript II KS (−), and the resulting *Sac*II–*Kpn* inserts were then transferred to the pHA-N1-90 vector, generating in frame fusions of all constructs to the HA epitope. To generate ΔN, the N-terminal domain was deleted by digesting with *Sac*II and *Bam*HI (which cuts 31 aa after the start of translation and 4 aa before DD1) and inserting a *Sac*II–*Bam*HI adaptor. To generate ΔDD1, a *Sac*II and *Ppu*MI digest was used to delete the whole N-terminal region through the end of DD1. The N-terminal domain was reinserted by PCR amplification with 5′ *Sac*II and 3′ *Ppu*MI tails. To generate ΔM, a

*Ppu*MI and *Cla*I (cutting 8 aa before DD2) digest was used to delete the middle domain, followed by insertion of a *Ppu*MI–*Cla*I adaptor, creating a linker of 13 aa between DD1 and DD2. ΔDD2 was generated by deleting DD2 and part of the C-terminal domain with a *Cla*I digest and reinserting the C-terminal domain by PCR. ΔDD1-ΔDD2 was generated by replacing the N-terminal half of ΔDD2 with that of ΔDD1 using the *Sac*II–*Mlu*I sites. ΔNLS2 was generated by overlap extension PCR, resulting in a 420 bp product flanked by *Sac*I and *Bam*HI sites, which was reinserted within the rest of the coding region. ΔM-ΔNLS2 NLS2 was generated by substituting the *Cla*I fragment from the C-terminal half of ΔM with that of ΔNLS2. N-DD1-M was generated by deleting DD2 and the C-terminal domain with a *Cla*I–*Kpn* digest. Reinserting DD2 as a PCR product in N-DD1-M resulted in the ΔC construct. We first attempted to express the DD1 and DD2 domains by themselves; these constructs were generated by PCR and inserted in the *Bgl*II–*Xho*I sites of pHA. To generate the N-DD1 and N-DD2 constructs, the N-terminal domain was amplified as a PCR product and inserted in *Eco*RI–*Bgl*II digested pHA-DD1 and pHA-DD2. The same PCR product was subcloned in a pHA *Eco*RI–*Bgl*II vector to generate the pHA-N construct. To generate N-DD1-DD2, DD1 was PCR amplified with a *Bgl*II site at the 5′ end and *Sal*I at the 3′ end. A 7-aa alanine linker was added to the 3′ end of DD1 with a *Sal*I–*Not*I adaptor. DD2 was amplified with a *Not*I site at the 5′ end and *Xho*I at the 3′ end and subcloned downstream of the DD1-Ala construct. The N-terminal domain was then added as an *Eco*RI–*Bgl*II insert as described above.

3xGFP constructs were generated as follows: EGFP was PCR amplified from a pEGFP-C1 (Clontech) template and inserted in a pUAST *Eco*RI–*Bgl*II vector to generate pUAST-GFP. Spe-GFP-Xba was generated by PCR and ligated in pUAST-GFP and a double insertion event was selected to obtain 3xGFP. NLS1 and NLS2 sequences were subcloned at the 3′ end of 3xGFP as *Xba*I–*Xho*I adaptors. DD1 was PCR amplified and subcloned in a 3xGFP *Xba*I–*Xho*I vector.

Transgenic animals were generated using standard procedures (Rubin and Spradling, 1982; Spradling and Rubin, 1982). At least three independent transgenic lines were obtained for each construct. The genotype of most rescue animals is *w; dac3*, *dpp-lacZ/dac^{GAL4}; UAS-HA-dacX/+*, where *X* denotes the constructs shown in Fig. 1 and Table 1. For analysis of mushroom body rescue, brains from *w*, *UAS-CD8-GFP; dac^{3}*, *dpp-lacZ/dac^{GAL4}; UAS-HA-dacX/+* animals were dissected. Synergy was assayed on animals of the following genotype: *w; UAS-HA-dacX/+; UAS-eya/dpp-GAL4*. For nuclear localization experiments, salivary glands of *AB1/+; UAS-3xGFP-Y/+* larvae were dissected, where *Y* is either NLS1, NLS2, or DD1 and *AB1* is a salivary gland-specific *GAL4* driver (courtesy of Mitzi Kuroda). *UAS-CD8-GFP* was obtained from the Bloomington Stock center and the *dpp-lacZ* reporter (Blackman et al., 1991), and *dpp-GAL4* (Staehling-Hampton and Hoffmann, 1994) alleles have been previously described. *UAS-eya* is a gift from F. Pignoni and L. Zipursky.

The *lacZ* P-element in *dac^{P}* (Mardon et al., 1994) was replaced with a *GAL4* P-element (*PGawB*) to generate *dac^{PG}* using a P-element replacement strategy previously described (Sepp and Auld, 1999). Since *dac^{PG}* causes only a weak phenotype, it was further subjected to a local hop screen to isolate a null *dac* allele, *dac^{GAL4}*. The local hop screen was performed by mobilizing *dac^{PG}* with *Δ2–3* transposase and selecting stronger w^{+} males (w^{++}) that also suppressed a gain-of-function allele of epidermal growth factor receptor, *Egfr^{Elp}*, phenotype. Since strong *dac* alleles are strong suppressors of *Egfr^{Elp}*, this strategy highly increased the efficiency of the local hop screen. w^{++} *Sup* (*Egfr^{Elp}*) animals were tested for complementation by crossing to a null allele of *dac*. Southern analysis was performed to molecularly characterize the *dac^{GAL4}* allele.

Sequencing of dac alleles

Dac mutant fly stocks were obtained from Kevin Moses and Iain Dawson. Heterozygous flies of 12 different *dac* alleles were crossed to *dac^{4}*, a small deletion that spans the entire *dachshund* locus (data not shown). *dac* mutant pharate pupae were isolated and phenotype was confirmed by dissection. Genomic PCR was performed with primers in the intronic regions around each exon using high-fidelity Platinum Pfx polymerase (Invitrogen). The PCR products were purified through MicroCon YM-100 spin columns. Purified product was sequenced using primers internal to the genomic PCR primers using ABI BigDye Terminator v3.0 Ready Reaction and analysis on an ABI 3100 sequencer. Sequence was analyzed using Sequencher 3.1.1 (GeneCo-

Table 1
Summary of rescue, nuclear localization, and synergy experiments

Construct	Rescue[a]	Nuclear[b]	Synergy[c]
HA-Dac^{F}	Yes	Yes	Strong
HA-ΔN	Yes	Yes	Medium
HA-ΔDD2	Yes	Yes	Medium
HA-ΔNLS2	Yes	Yes	Medium
HA-ΔM	Yes	Yes	Medium
HA-ΔM-ΔNLS2	Yes	Yes	ND
HA-ΔC	Yes	Yes	Medium
HA-N-DD1-DD2	Yes	Yes	Medium
HA-N-DD1-M	Yes	Yes	Medium
HA-ΔDD1	No	Partial	Weak
HA-ΔDD1-ΔDD2	No	Partial	None
HA-N-DD1	No	Yes	None
HA-N-DD2	No	Yes	None
HA-N	No	Partial	ND

[a] Rescue is the same for all tissues and is considered as a "yes" or "no" event here.
[b] Yes means that the majority of the protein is found in the nucleus. Partial means that the protein is equally distributed in the nucleus and cytoplasm.
[c] Strong = ectopic eyes on leg and thorax; medium = larger and more penetrant eye induction ventral to the antenna; weak = red pigmentation on the dorsolateral side of the antenna with no ommatidia; ND = not determined.

des). All suspected mutations were confirmed from independent genomic DNA preparations and PCR. All primer sequences are available upon request.

Immunohistochemistry

Imaginal discs, salivary glands, and adult brains were dissected and stained as described (Davis et al., 2003; Mardon et al., 1994). Live GFP was monitored in rescued brains after a 30-min 4% paraformaldehyde/40 mM lysine/PBS (PLP) fix and in *AB1; 3xGFP* salivary glands after a 10-min 4% formaldehyde in PBS fix. Antibodies were used at the following dilutions: rabbit anti-HA (Santa Cruz Biotechnology) at 1:10; mouse anti-Dac (2–3) (Mardon et al., 1994) at 1:200; rat anti-ELAV (Robinow and White, 1991) at 1:200; rabbit anti-β-gal (Cappel) at 1:800; mouse anti-Glass (Moses and Rubin, 1991) at 1:200; ALEXA 488 goat anti-rabbit and goat anti-rat (Molecular Probes) at 1:500; Cy3 goat anti-mouse and goat anti-rabbit (Jackson Immunochemicals) at 1:500; and HRP goat anti-mouse (Jackson Immunochemicals) at 1:200. Rabbit anti-HA and anti-β-gal antibodies were preabsorbed with methanol fixed embryos (rehydrated through a PBS–EtOH dilution series) for 2 h at room temperature. Fluorescently stained discs were mounted in Vectashield and images were captured with a Zeiss LSM 510 confocal microscope. DAB-stained discs were mounted in 80% glycerol, 20% PBS, and images were captured with a Hamamatsu C5810 camera.

Scanning electron microscopy, histology, and 3-D color photography

Adult flies were prepared for electron microscopy as described (Kimmel et al., 1990). Adult fly heads were embedded in Durcapan Resin (Fluka) and sectioned as described (Tomlinson and Ready, 1987). Sections (1.5 μm) were dried briefly at 80°C, stained with 1% toluidine blue, 1% borax, and mounted in Cytoseal XYL (Stephens Scientific). Sections were analyzed by DIC microscopy and images were captured with a Hamamatsu C5810 camera. Color pictures of adult eyes were captured with a Leica MZ16 stereomicroscope and processed with Image-Pro Plus image analysis software.

Results

To elucidate the function of DD1, DD2, and other portions of the Dac protein, we devised four in vivo assays. First, we set up a rescue assay system where dac^{GAL4} is used to drive expression of a series of *UAS-dac* transgenes (Fig. 1) in a *dac* null mutant background to determine which domains are essential for Dac function. Efficiency of rescue was assessed in the eye, leg, and brain structures where consequences of loss of *dac* function are most drastic. Second, we characterized the molecular nature of 11 preexisting hypomorphic and null mutations in *dac* with the intent of uncovering domains and amino acids critical for Dac function. Third, based on prior knowledge that *dac* and *eya* synergize to induce ectopic eye development, we assessed the requirement for different Dac domains for this synergy in vivo. Finally, since Dac is a large nuclear protein (approximately 120 kDa), we tested whether specific domains are necessary or sufficient for nuclear localization in salivary gland cells, which are large and where protein localization can be readily and precisely visualized.

The dac^{GAL4} rescue assay

Our rescue assay required a GAL4 driver that faithfully reproduces the endogenous *dac* pattern of expression in a *dac* null mutant background. We employed a P-element replacement strategy to substitute the *lacZ*-containing P-element of insertion line dac^{P} with a *PGawB* element, which contains the *GAL4* gene (Sepp and Auld, 1999). The resulting *GAL4* insertion line (dac^{PG}) displays a weak *dac* phenotype that is even less severe than hypomorphic dac^{P} allele. To create a *dac* null mutant expressing *GAL4* in the *dac* pattern, dac^{PG} was further subjected to a local hopping screen to generate dac^{GAL4}. Southern and PCR analyses of dac^{GAL4} DNA reveal the presence of an intact P-element near the transcription initiation site followed by a deletion encompassing the entire coding region of *dac* (data not shown). The expression pattern of this *GAL4* insertion was compared to that of endogenous *dac* (Mardon et al., 1994). Wild-type *dac* expression in the eye imaginal disc precedes the morphogenetic furrow (MF) and continues to be expressed in photoreceptors R1, R6, and R7 for a few columns posteriorly (Fig. 2A and data not shown). In the leg disc, *dac* is expressed in a ring of tissue that gives rise to the femur, tibia, and first three tarsal segments of the adult leg (Fig. 2B). *dac* expression in the brain is first detected in the embryo and continues into adult life. In the adult brain, *dac* is expressed in the Kenyon cells, which send axons deeper into the brain to form a structure called the mushroom body (MB) that is implicated in learning and memory (Fig. 2C) (Kurusu et al., 2000; Martini et al., 2000; Noveen et al., 2000). *dac* is also expressed in a crescent in the antennal disc (Fig. 2A) and in a complex pattern in the wing disc (Fig. 2D). Furthermore, *dac* is expressed and differentially regulated in male versus female genital discs (Figs. 2E and G) (Keisman and Baker, 2001). To determine whether the expression pattern of dac^{GAL4} coincides with the endogenous *dac* pattern, we crossed dac^{GAL4} to *UAS-HA-N-DD1* transgenic animals that express an HA-tagged Dac protein missing the middle, DD2, and C-terminal domains. Expression of this construct does not cause any readily observable phenotype and does not alter endogenous *dac* expression when driven by dac^{GAL4} (data not shown). Since our monoclonal Dac antibody is raised against the middle domain of Dac, we were able to costain imaginal

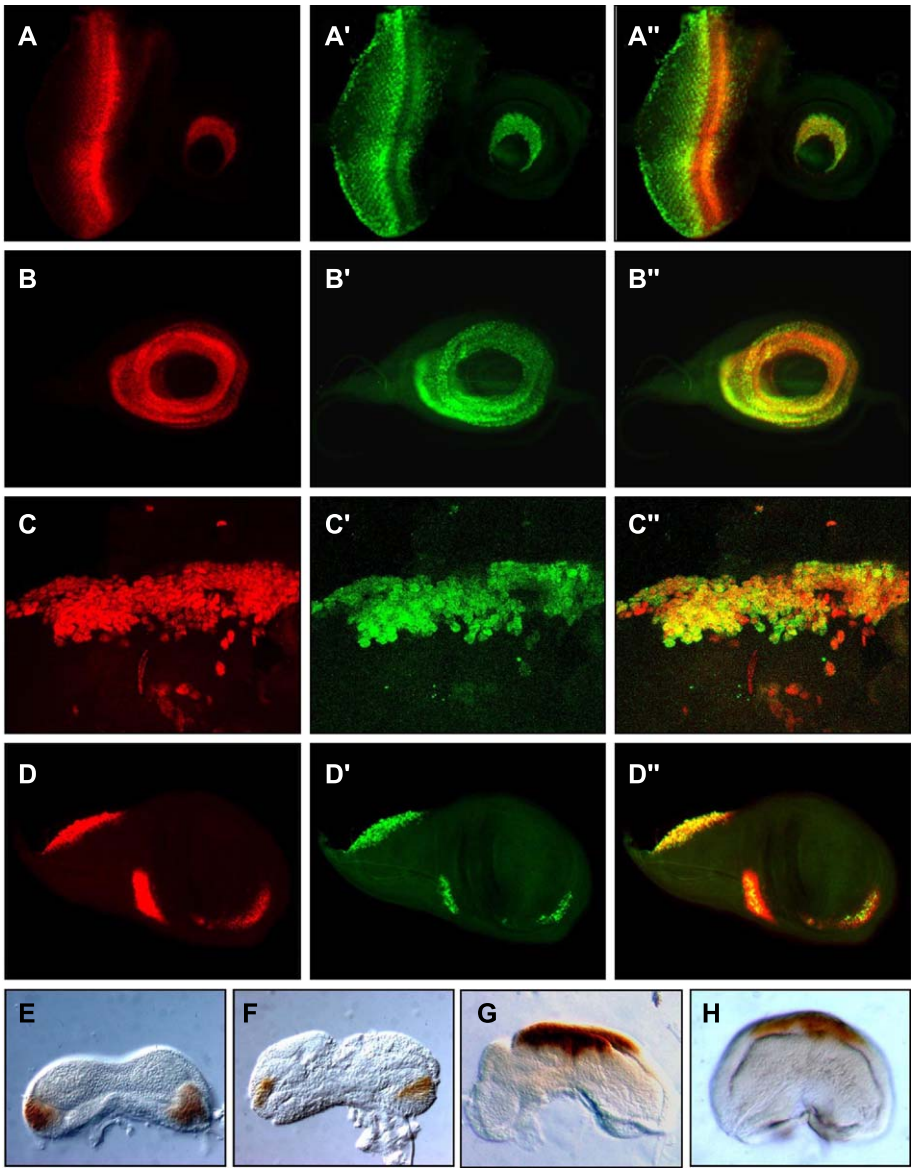

Fig. 2. dac^{GAL4} faithfully reproduces the endogenous *dac* expression pattern. Third instar eye (A) and leg (B) discs, adult brains (C), and wing discs (D) from dac^{GAL4}/+; *UAS-HA-N-DD1*/+ animals were costained with α-Dac (red) and α-HA (green). Merge of the two channels is shown in the third column. α-Dac recognizes the middle domain of Dac, which is missing in HA-N-DD1. Panels E–H show horseradish peroxidase diaminobenzidine (HRP-DAB) staining of third instar male (E and F) and female (G and H) genital discs, with either α-Dac (E and G) or α-HA (F and H). Posterior is to the left in (A) and to the top in (B and D); dorsal is to the top in (C); anterior is to the top in (E–H).

discs and adult brains with anti-HA and anti-Dac antibodies to monitor GAL4 and Dac patterns simultaneously. HA-N-DD1 is localized to the nucleus as is wild-type Dac, thus allowing precise assessment of colocalization. We found that dac^{GAL4} recapitulates the wild-type *dac* expression pattern in all of the tissues described above (Fig. 2). Although HA staining in the eye coincides with that of Dac anterior to the MF, it continues to be expressed in posterior cells longer than endogenous Dac (Figs. 2A–A″). A similar pattern was observed using a full-length UAS-HA-Dac construct (data not shown), suggesting that the perdurance of HA-Dac staining in cells posterior to the MF is likely to be the result of perdurance of GAL4 protein.

DD1 is the only domain essential for Dac function

Our initial approach to investigating the function of different Dac domains was to make systematic single-domain deletion constructs and test their ability to rescue *dac* null phenotypes. In these constructs, only one domain is deleted at a time (i.e., N-terminal domain, DD1, middle domain, DD2, or C-terminal domain) while the rest of the protein is kept intact. Since we suspected that a putative

NLS sequence within DD2 might be important for nuclear localization, we kept this sequence in the ΔDD2 construct and deleted this NLS alone in a separate construct (ΔNLS2) to test its function. We included an N-terminal HA tag in all constructs to detect the pattern and level of expression of each unambiguously.

All rescue assays were performed in dac^{GAL4}/dac^{3} background, where dac^{3} is a phenotypic null allele resulting from a large insertion (>25 kb) in intron 2 (data not shown). Since dac^{3} homozygous mutant imaginal discs are Dac null by antibody staining, we believe that the insertion in intron 2 results in early truncation of the protein or transcript destabilization (Fig. 4A and data not shown).

In general, rescue appears to be an all-or-none event. Different constructs either fully rescued all *dac* mutant phenotypes (or nearly so) or no rescue was observed in any tissue. We determined that a full-length Dac protein with an N-terminal HA tag is capable of full rescue of all Dac phenotypes (Figs. 3A–C, E–G, I–K, M–O, and Q–S; compare dac^{F} to wild-type and null panels). We detect no difference between rescue with an untagged Dac and HA-tagged Dac, suggesting that the presence of an HA tag does not compromise Dac function. Furthermore, all single-domain deletion *UAS* transgenes rescue all *dac* phenotypes, except for ΔDD1, which is a functional null, suggesting that DD1 might be the only domain essential for Dac function (Table 1 and data not shown). To verify these results and determine the smallest construct capable of rescue, we generated additional constructs expressing DD1 alone, DD2 alone, or DD1-DD2 connected by a 7-aa alanine linker. Despite testing more than 10 transgenic lines for each construct, we were not able to detect these proteins by immunohistochemistry, suggesting that they may not be stable proteins. In an effort to overcome this problem, we added the N-terminal domain to all three constructs, thus generating N-DD1, N-DD2, and N-DD1-DD2. All of these constructs are detectable at high levels and localize to the nucleus properly, suggesting that the N-terminal domain is sufficient to stabilize these proteins. Only N-DD1-DD2 rescues *dac* null phenotypes but not N-DD1 or N-DD2. Since the single-domain deletion results pointed to DD1 as the only domain essential for Dac function, we wondered if the inability of N-DD1 to rescue is due to absence of a stabilizing sequence at its C-terminus. In accordance with this idea, N-DD1-M is also able to rescue *dac* null phenotypes. Since ΔN, ΔM, and ΔDD2 all rescue *dac* phenotypes, the N-terminal, DD2, and middle domains do not have any essential function of their own. Instead, their presence in N-DD1-M and N-DD1-DD2 may help stabilize DD1 as a functional domain. Control constructs ΔDD1-ΔDD2 and N alone did not rescue *dac* null phenotypes, indicating that none of these domains is sufficient to provide *dac* function. Since DD2 is a highly conserved domain, we predicted that DD2 would also be important for Dac function in at least some tissues. Surprisingly, we find that within the confines of our rescue assay, DD2 is not absolutely required for Dac function (Figs. 3D, H, L, P, and T and Table 1).

To assess the potential rescue activity for all constructs, we systematically checked all tissues where *dac* null mutants display a prominent phenotype. Dac plays an important role in early retinal determination of the eye. The wild-type *Drosophila* eye is composed of a regular array of 750–800 unit eyes called ommatidia (Fig. 3A). Transverse sections through the eye show the internal organization of each ommatidium with light-sensing rhabdomeres of each photoreceptor arrayed in a trapezoidal shape (Fig. 3E). Complete loss of *dac* function results in animals that have little or no eye (Fig. 3B), comprising 0–15 ommatidia (Mardon et al., 1994). Sections through these ommatidia show a highly disorganized structure with few visible rhabdomeres (Fig. 3F). Rescue with different deletion constructs revealed one of two phenotypes: either there was no rescue of the eye or it was rescued to a size that is nearly wild type (comprising 550–700 ommatidia) with excellent overall organization but some posterior roughness (Figs. 3C and D). We observed some variability in the degree of rescue by different insertions of each construct. For example, one allele that gave a particularly rough phenotype at 25°C improved drastically upon raising animals at 18°C, suggesting that higher levels of Dac can contribute to some of the disorganization we observe. Transverse sections through the rescued eyes reveal that their internal structure is mostly morphologically wild type, with occasionally disorganized ommatidia (Figs. 3G and H and data not shown). We monitored development of the eye disc by visualizing the neuronal marker ELAV and the morphogenetic furrow marker *dpp-lacZ*. In wild-type discs, growing clusters of ommatidia develop posterior to the MF; whereas in *dac* null eye discs, the MF does not initiate its anterior movement and very few or no photoreceptors differentiate (Figs. 3I and J). In rescued eye discs, the ELAV pattern is disrupted to varying degrees. Specifically, spacing between ommatidia is not uniform in most rescue discs (Figs. 3K and L), and this may account for the posterior roughness observed in many adult eyes.

In the brain of *dac* null mutants, the mushroom body displays a thinning of the vertical α-lobes and disorganization of the lateral lobes (β/β′ and γ) (Martini et al., 2000). Full-length Dac rescue brains have more organized MB structures with thicker α-lobes. Although organization of the lateral lobes is improved, full rescue was not observed. Nevertheless, the degree of rescue is consistent among different constructs, and the absence of DD2 does not significantly affect rescue capability (Figs. 3M–P).

dac mutant legs are truncated due to a merge of the femur, tibia, and upper tarsal segments into a small, poorly defined tissue mass (Mardon et al., 1994). Full-length Dac and other rescue constructs that include a stabilized DD1 restore proper segmentation of the leg. In all rescued legs, the femur, tibia, and five tarsal segments are clearly visible. The overall size of the leg is also close to normal, although

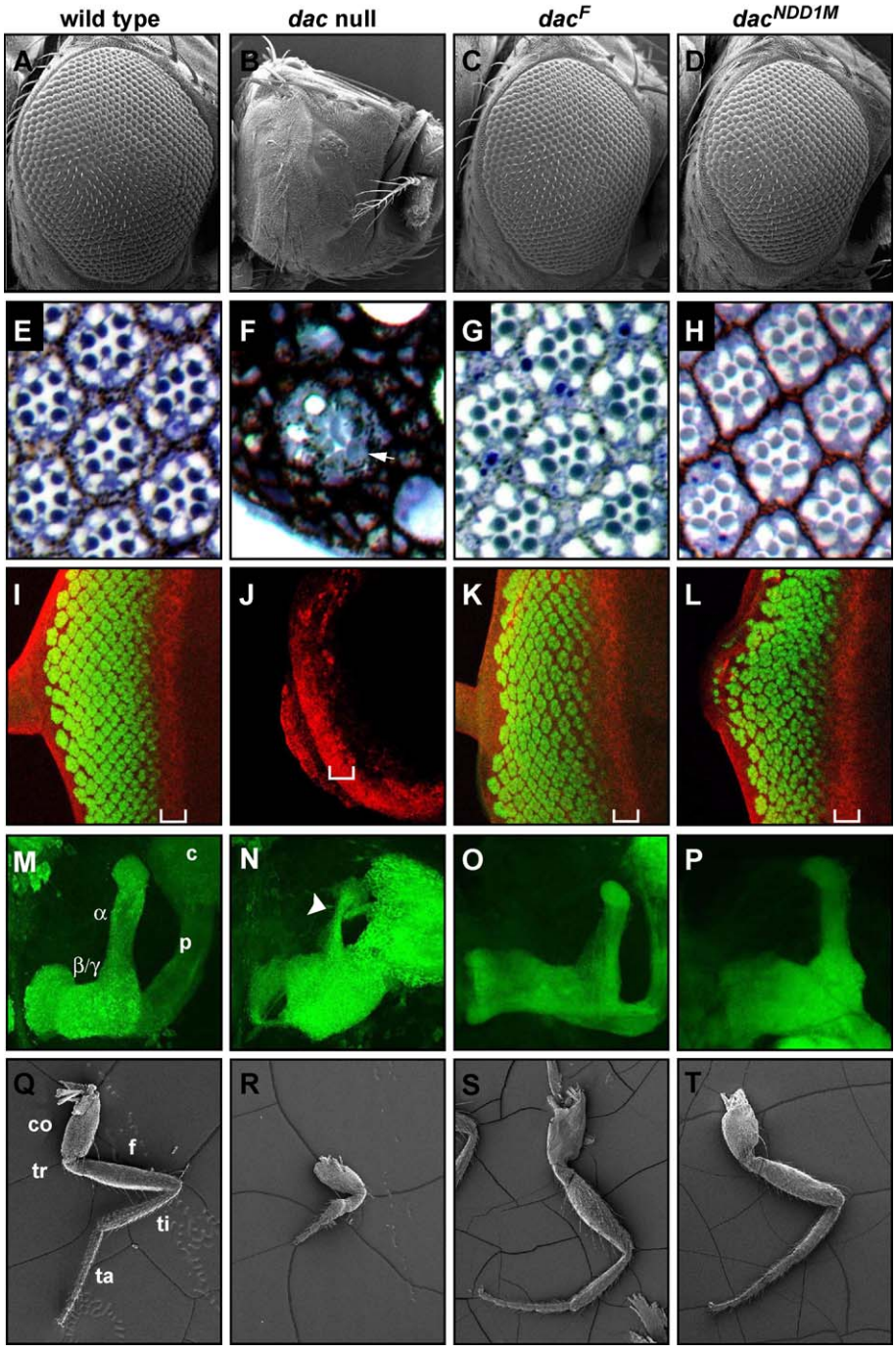

Fig. 3. DD1 is the only domain essential for Dac function. Rescue animals were compared to wild-type (first column on the left) and *dac* null (dac^{GAL4}/dac^{3}) animals (second column). Full-length Dac rescues null phenotypes in all tissues examined (third column). N-DD1-M rescue is shown as an example of a construct lacking DD2, yet rescuing all null phenotypes (fourth column). We examined the external morphology and size of the eye on SEM images (A–D). Ommatidial organization is revealed through transverse plastic sections (E–H). The arrow in (F) indicates disorganized rhabdomeres in a single ommatidium of a *dac* null eye. Photoreceptor development is monitored by staining against the neuronal marker ELAV (green) and the morphogenetic furrow marker *dpp-lacZ* (red) in third instar eye imaginal discs (I–L). MF position is indicated by a bracket in panels I–L. Posterior is to the left in all eye pictures. Even though N-DD1-M rescue shows significant disorganization in the developing eye disc (L), the adult eye has only very minor abnormalities (D and H). Mushroom body structure was observed by expressing *UAS-CD8-GFP* along with *UAS-dac* rescue constructs (M–P). In (panel M), MB structures are denoted as α = vertical α lobes; β/γ = horizontal β and γ lobes; p = peduncle; and c = calyx. The arrowhead in panel N points to a *dac* null α lobe, which is much thinner than wild type. Also note the highly disorganized β/γ lobes. Adult leg morphology is seen in panels Q–T. In panel Q, adult leg segments are denoted as co = coxa; tr = trochanter; f = femur; ti = tibia; and ta = tarsal segments.

some small variations are observed among different rescue alleles (Figs. 3Q–T).

dac null mutants also display more subtle phenotypes in the adult antenna and genital structures in accordance with its expression pattern in the antennal and genital discs. The wild-type antenna is composed of six segments and *dac* mutants have a defective joint between the fifth and sixth segments (Dong et al., 2002). Since this phenotype is rather subtle, we did not score animals for its rescue. In addition, loss of *dac* function results in a reduced clasper, a structure on the outer surface of male genitalia implicated in stabilizing female genitalia for successful mating. Furthermore, *dac* mutant females display a fusion of ducts connecting the two spermethecae to the uterus (Keisman and Baker, 2001). Although we did not specifically determine rescue of these phenotypes in our assays, we did observe that all rescue males and females are fertile (data not shown).

Mutations disrupting DD2 function display weak to moderate phenotypes

To further elucidate the function of specific Dac domains, we also analyzed the molecular nature of several hypomorphic and null mutant alleles of *dac*. Results of these analyses are summarized in Fig. 4. We found that nearly all nonsense mutations truncating Dac before or within the amino-terminal portion of the middle domain result in a null phenotype. The sole exception is dac^{3CX1}, which encodes a stop codon at Q125 and displays a severe but not null *dac* mutant phenotype. Staining of dac^{3CX1} mutant discs with an anti-Dac antibody that recognizes the middle portion of the protein revealed weak and disorganized Dac expression, suggesting that there may either be an alternative start site or some other mechanism by which translation continues beyond the termination signal (data not shown). It is interesting to note that similar to the phenotypic null allele dac^{8}, which truncates just 14 aa downstream of DD1, our N-DD1 construct is not sufficient to rescue any *dac* phenotypes and the shortest constructs capable of rescue are N-DD1-DD2 and N-DD1-M.

In addition to the nonsense mutants discussed above, we analyzed five hypomorphic alleles of *dac*. Two of these alleles, dac^{10FA3} and dac^{6}, map to single amino acid changes in conserved residues of DD1 (V290I and L304F, respectively). These animals display a severe phenotype with very small, disorganized eyes (one fourth to one fifth of a wild-type eye), and almost null legs, indicating that residues V290 and L304 are important for proper function of the DD1 domain. We mapped dac^{5}, a hypomorphic allele, to Q645X, where a C > T base change results in a nonsense mutation and truncation 42 aa upstream of DD2. In addition, dac^{3BF1} (another hypomorphic allele) maps to Q797X, again a C > T base change terminating the protein 51 aa into DD2. Although both alleles encode proteins that are truncated before or within DD2, they display only moderate *dac* phenotypes. The adult eye is present but about half the size of a wild-type eye with an outer morphology that appears mildly disorganized (Figs. 5A and E). Sections through these eyes indicate that the trapezoidal rhabdomere structure is mostly preserved with a small percentage of ommatidia abnormally constructed (Figs. 5B and F). Staining of eye discs with the

A

dac Allele	Mutation	Base Change	Phenotype
3CX1	Q125X	C > T	Severe
10BAL	Q140X	C > T	Null
12CN1	Q178X	C > T	Null
1	Q225X	C > T	Null
BDD1	Q276X	C > T	Null
10FA3	V290I	G > A	Severe
6	L304F	C > T	Severe
8	Q351X	C > T	Null
5	Q645X	C > T	Moderate
3BF1	Q797X	C > T	Moderate
2	E816K	G > A	Weak
3	> 25 Kb insertion	NA	Null

B

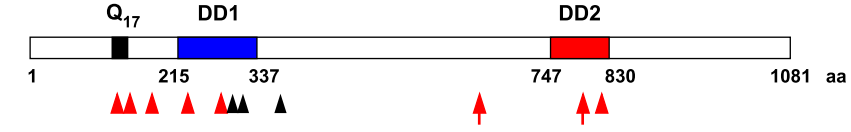

Fig. 4. Molecular analysis of *dac* mutant alleles. Panel A shows a list of twelve *dac* mutant alleles with identified base and amino acid changes and their associated phenotypes. A severe phenotype is defined as an eye that is one fourth to one third the size of wild type and an almost null leg; a moderate phenotype indicates that the eye is half the size of wild type while the leg is two thirds the size of normal; a weak phenotype indicates that the eye is 75% the size of wild type with some disorganization and the leg is 75% the size of wild type with tibia-tarsal fusions. The >25 kb insertion in dac^{3} is in intron2. Panel B shows a schematic of Dac protein with the positions of *dac* mutant alleles shown with arrowheads. Red arrowheads indicate nonsense mutations and black arrowheads denote missense mutations. The two red arrows indicate dac^{5} (left arrow) and dac^{3BF1} (right arrow), which are discussed in detail in Fig. 5.

neural marker ELAV reveals some disorganization in developing photoreceptor clusters (Figs. 5C and G). Moreover, dac^{5} and dac^{3BF1} mutant legs have a recognizable femur and tibia and up to four tarsal segments, although they appear malformed and are about half the size of a wild-type leg (Figs. 5D and H). Finally, dac^{2}, which maps to a missense mutation in a conserved residue of DD2 (E816K), displays phenotypes similar to but weaker than dac^{5} and dac^{3BF1}. All three *dac* alleles affecting DD2 are expressed at levels comparable to wild type, suggesting that the mild mutant phenotypes observed in these animals is a result of loss of DD2 function and is not due to a reduction in protein levels (Figs. 5I–L). Interestingly, the N-DD1-M construct, which is very similar in composition to dac^{5} and dac^{3BF1}, is capable of fully rescuing *dac* phenotypes, suggesting that DD2 function can be compensated for by overexpression of constructs lacking DD2.

Dac and Eya synergize in the absence of DD2

Dac and Eya are part of the RD network that is necessary and sufficient for retinal development (Chen et al., 1999). Ectopic expression of either Dac or Eya with the *dpp-GAL4* driver is sufficient to induce ectopic eye tissue to a small extent and at low penetrance (Chen et al., 1997). Ectopic expression of Eya results in red pigmentation ventral to the antenna with occasional ommatidial formation in approximately 30% of animals observed (Fig. 6A). Similarly, ectopic expression of Dac results in small patches of eye ventral to the antenna (Fig. 6C). However, when coexpressed, these two genes act synergistically to form large patches of ectopic eye tissue ventral to the antenna that often fuses to and expands the wild-type eye (Fig. 6E). In addition, ectopic eye formation is also observed on the legs and thorax with complete penetrance (Chen et al., 1997). In vitro studies, including yeast two-hybrid and GST pull-down assays, suggest that Eya and Dac physically interact through conserved domains (DD2 in Dac and ECD1 in Eya) (Chen et al., 1997). An important question then is to determine whether the physical interaction between these two proteins is required for the genetic synergy observed. Surprisingly, we continue to observe some synergy between Eya and ΔDD2, and Eya and N-DD1-M, where both Dac constructs lack DD2 (Fig. 6G and data not shown). Indeed, we find that all constructs capable of rescuing *dac* phenotypes also synergize with

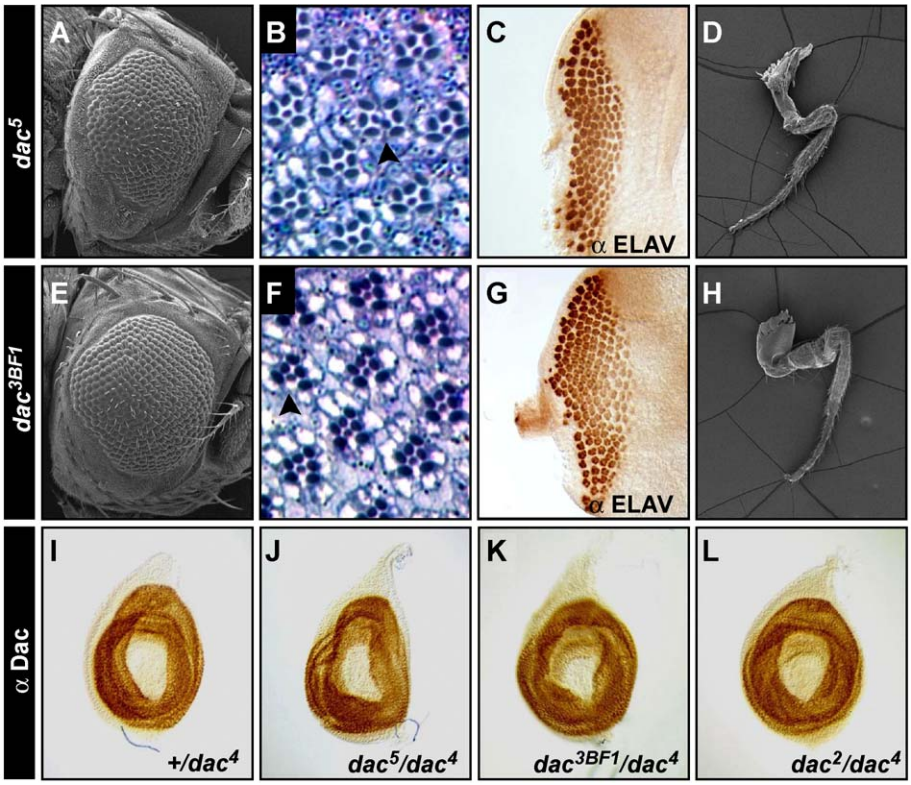

Fig. 5. Loss of DD2 function causes a moderate *dac* phenotype. Eye and leg phenotypes of dac^{5} (A–D) and dac^{3BF1} (E–H) animals, which encode Dac proteins that truncate before or within DD2 (see schematic in Fig. 4). SEM images of dac^{5} and dac^{3BF1} adult eyes (A and E) show some disorganization and size reduction (compare to Fig. 3A). Sections through these eyes reveal occasional abnormal ommatidia with either extra (arrowhead in B) or missing (arrowhead in F) rhabdomeres (B and F). Staining of mutant developing eye discs with the neural marker ELAV also reveals a mild disorganization of ommatidial clusters (C and G). dac^{5} and dac^{3BF1} legs are about two thirds the length of a wild-type leg (compare to Fig. 3Q), each possessing a recognizable coxa, femur, tibia, and up to four tarsal segments (D and H). Dac staining of wild-type and *dac* mutant third instar leg imaginal discs shows similar levels of protein expression (I–L). Posterior is to the left in all panels.

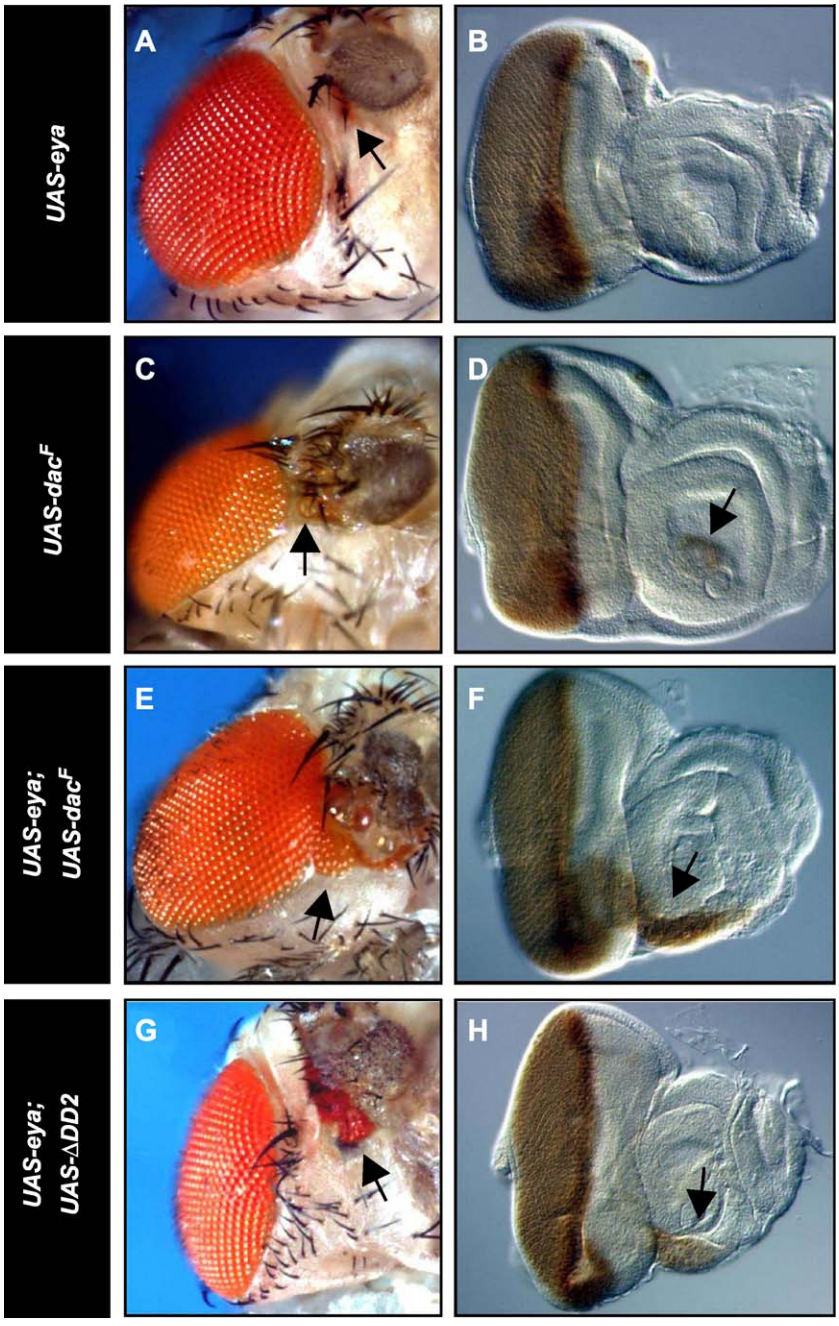

Fig. 6. Dac and Eya can synergize to induce ectopic eye development in the absence of DD2. The eye-antennal region from adult flies (left column) and DAB staining against the photoreceptor marker Glass in third instar eye-antennal discs (right column) are shown. Posterior is to the left in all eye discs. Synergy experiments were conducted using *dpp-GAL4* to drive combinations of *UAS-eya* and different *UAS-dac* transgenes. *UAS-eya* (A and B) or *UAS-dac^F* (C and D) are capable of inducing only red pigmentation (arrow in A) or small ectopic eyes (arrow in C) with low penetrance. Arrow in D points to a weak patch of ectopic Glass staining. (E and F) When expressed together, Eya and Dac induce large and 100% penetrant ectopic eyes ventral to the antenna (arrow in E) and Glass staining expands into the antenna in eye-antennal discs (arrow in F). Synergy is observed with 100% penetrance with all Dac constructs that are capable of rescuing *dac* null phenotypes, although none of these constructs (except for full-length Dac) can induce ectopic eye formation when expressed alone. Panels G and H show synergistic interaction between *eya* and *ΔDD2*, resulting in a large patch of ectopic eye ventral to the antenna in adults (arrow in G) and expansion of Glass staining expands toward the antenna in larval discs (arrow in H).

Eya to induce ectopic eye development. More specifically, we find that deletion of any Dac domain reduces the efficiency of synergy such that ectopic eye formation is limited to the ventral antenna and is never present on the leg or thorax. However, ectopic eyes formed ventral to the antenna are larger than those expected by simple addition of the effects of either Dac or Eya alone, therefore suggesting synergy (results summarized in Table 1). This synergistic effect is even more striking since, except for full-length Dac, none of the Dac construct alleles we tested

can induce ectopic eye formation by themselves (data not shown).

Synergy between Eya and Dac constructs is evident in the developing eye-antennal disc as well. While staining of the photoreceptor-specific marker Glass is normally detected only posterior to the MF, co-misexpression of Eya and Dac results in an extension of Glass staining toward the antenna (Figs. 6F and H). Expression of Eya or Dac alone does not disrupt the Glass pattern significantly, except for the appearance of an occasional weak patch in the antenna (Figs. 6B and D and data not shown). As expected, no synergy is observed between Eya and ΔDD1. However, a small red pigment patch (with no detectable ommatidia) is present on the antenna of 100% of the animals expressing Eya and ΔDD1, suggesting that a weak interaction may still exist between these proteins (data not shown).

Dac contains multiple domains sufficient for nuclear localization

All nuclear proteins translocate to the nucleus from the cytoplasm where they are synthesized. The nucleus is separated from the cytoplasm by the nuclear envelope, which allows free diffusion of molecules up to approximately 60 kDa in size through its nuclear pore complexes (NPC). Proteins that are larger than 60 kDa can translocate to the nucleus by active transport through the NPC (Gorlich and Kutay, 1999). Since Dac is a nuclear protein of 120 kDa and thus too large to enter the nucleus by passive diffusion, we envisioned two ways in which it can translocate to the nucleus. First, a nuclear localization signal (NLS) within Dac itself may target it to the nucleus through the NPC. Second, Dac may bind other proteins, which are targeted to the nucleus by their own NLS sequences, and use this interaction to move from the cytoplasm to the nucleus. Nuclear localization signals are typically short stretches of mostly basic residues that target a protein for active transport into the nucleus (Gorlich and Kutay, 1999). PSORTII protein motif recognition software indicates two possible NLS sequences in Dac. The first (NLS1) is a basic motif (PQLKKHR) 15 aa downstream of DD1 (aa 353–359), whereas the second (NLS2) is a bipartite motif (RKLRVLYQKRFRRERKI) residing in DD2 (aa 803–819) (schematic in Fig. 7). We tested these putative NLS sequences for sufficiency by fusing them to the C-terminus of a 3xGFP construct. The 3xGFP construct consists of three consecutive GFP molecules (a GFP::GFP::GFP fusion) such that the resulting protein is predicted to be 72

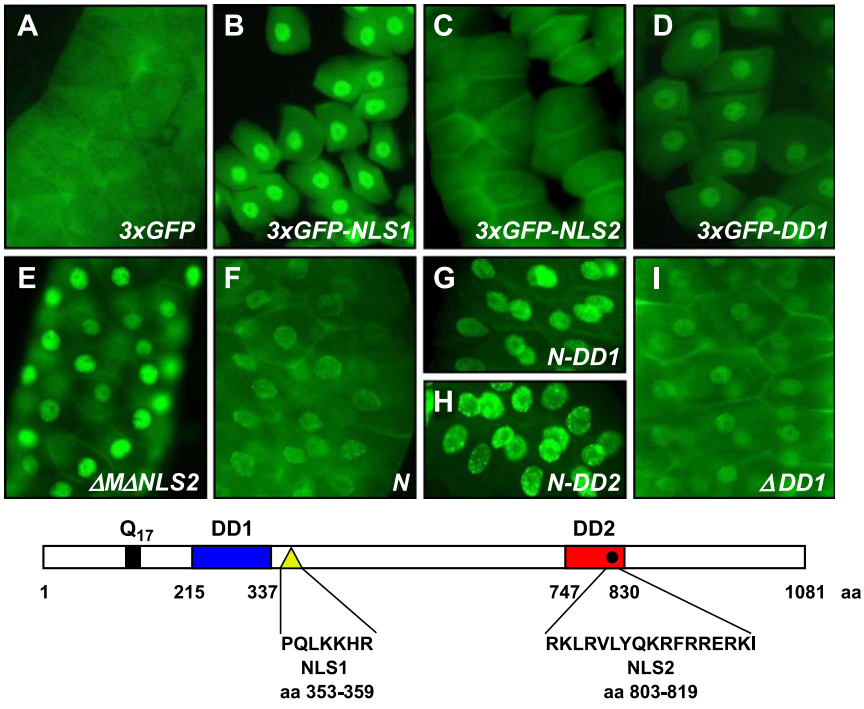

Fig. 7. DD1, DD2, and a basic NLS in the middle domain are each sufficient to translocate Dac into the nucleus while only DD1 is necessary for complete nuclear localization. (A–D) Live GFP is detected in salivary gland cells after a mild fix. Salivary glands from *AB1/+; UAS-3xGFP/+* (A), *AB1/+; UAS-3xGFP-NLS1/+* (B), *AB1/+; UAS-3xGFP-NLS2/+* (C), and *AB1/+; UAS-3xGFP-DD1/+* (D) third instar larvae (where *AB1* is a salivary gland-specific *GAL4* driver) are shown. 3xGFP is uniformly distributed between the nucleus and cytoplasm (A). Both NLS1 (B) and DD1 (D) are sufficient to cause an increase in nuclear localization of 3xGFP whereas NLS2 (C) is not. (E–I) HA-tagged Dac constructs are detected by α-HA antibody staining in salivary gland cells. Animals of the following genotypes are shown: *AB1/+; UAS-ΔMΔNLS2/+* (E), *AB1/+; UAS-N/+* (F), *AB1/+; UAS-N-DD1/+* (G), *AB1/+; UAS-N-DD2/+* (H), and *AB1/+; UAS-ΔDD1/+* (I). Deletion of both predicted NLS signals does not alter protein localization significantly (E). The N-terminal domain is uniformly distributed in cells (F), whereas N-DD1 and N-DD2 are nuclear (G and H). Deletion of DD1 results in a higher cytoplasmic distribution (I). The schematic shows the position and sequence of PSORTII-predicted NLS sequences.

kDa and hence, in theory, beyond the simple diffusion limit. To precisely determine subcellular localization, we wanted to express our transgenes in sufficiently large cells where the nucleus and cytoplasm can be easily distinguished. The third instar larval salivary gland provides the ideal cells for this purpose. We used the *GAL4* line *AB1* to express our *UAS-3xGFP* constructs specifically in the salivary gland. Although we expected the 3xGFP protein to be exclusively cytoplasmic, we observe GFP fluorescence uniformly distributed in the nucleus and cytoplasm (Fig. 7A). Nevertheless, we find that 3xGFP-NLS1 strongly localizes to the nucleus, whereas 3xGFP-NLS2 is indistinguishable from 3xGFP alone (Figs. 7B and C). We conclude that NLS1 is sufficient for nuclear localization while NLS2 is not. This result is somewhat surprising since ΔM, which deletes NLS1 along with the rest of the middle domain of Dac, can rescue the null phenotype (Table 1). Indeed, we find that ΔM is nuclear when expressed in the salivary gland as detected by anti-HA antibody staining. Moreover, ΔNLS2 and ΔM-ΔNLS2 proteins are also nuclear and rescue *dac* null phenotypes as well (Fig. 7E and data not shown). Therefore, we analyzed other rescue constructs for nuclear localization and determined that the presence of either DD1 or DD2 is also sufficient for Dac protein to translocate to the nucleus (Table 1). More specifically, we find that the N-terminal domain is small enough to diffuse into the nucleus but is also present in the cytoplasm at equally high levels. However, both N-DD1 and N-DD2 localize exclusively to the nucleus, suggesting both DD1 and DD2 are sufficient for nuclear localization (Figs. 7F–H). Furthermore, we tested DD1 outside of its natural context by fusing it to the C-terminus of 3xGFP and found that it is sufficient for nuclear transport in that context as well (Fig. 7D). To determine whether DD1, DD2, and NLS1 are redundant for nuclear targeting, we examined the subcellular localization of all deletion constructs in salivary gland cells. Since N-DD1-M is completely nuclear, we find no special requirement for DD2. Similarly, since ΔM is nuclear, NLS1 is likely to be redundant with other domains. However, ΔDD1 does localize to both the nucleus and cytoplasm, suggesting that DD1 may be the domain primarily responsible for nuclear localization (Fig. 7I). While there are no NLS sequences predicted by PSORTII in DD1, we tested a short sequence at the C-terminus of DD1 with some similarity to a known NLS structure (composed of three basic amino acids surrounded by Proline residues) for nuclear targeting. However, we find that this sequence is not sufficient for nuclear transport when fused to the C-terminus of 3xGFP (data not shown). Therefore, more and perhaps all of the entire DD1 domain may be required for nuclear localization.

Discussion

Dac is a highly conserved protein involved in development of many diverse structures such as the eyes, legs, and brain in *Drosophila*. We conducted structure–function studies to determine whether the different conserved domains within Dac behave as independent functional modules with tissue-specific functions or if they collaborate toward one function. Our studies could not assign a function to the conserved stretch of CAG sequence encoding polyglutamine within the N-terminal domain. The full rescue observed with ΔN indicates that polyglutamine does not have any essential function. However, we cannot rule out a subtle function for this domain or for the nonconserved N-terminal, middle, and C-terminal domains since GAL4-driven high levels of expression in our rescue assays may compensate for the lack of these domains. In contrast, our studies have been successful in assigning and characterizing DD1 and DD2 functions. We find that the essential function of Dac is executed by DD1, while DD2 assists DD1 so that the protein can perform at its full capacity. Therefore, DD1 and DD2 appear to collaborate to perform one function. In addition, we find that DD1 is essential for proper nuclear localization, even though other domains are likely to contribute as well.

DD1 is the domain critical for Dac function

Our studies suggest that DD1 is the critical domain of Dac, meaning that it performs the essential function of the protein. We draw this conclusion from several observations. First, DD1 is highly conserved across species, suggesting that it performs an important function. Second, DD1 is the only domain essential for Dac function in our rescue assays, while all other domains are dispensable, including the second conserved domain, DD2. Third, missense mutations within DD1 result in severe *dac* mutant phenotypes, again indicating that DD1 function is critical. Fourth, all DD1-containing constructs are capable of synergizing with Eya to induce ectopic eyes. Despite all of these findings indicating the importance of DD1, DD1 alone is not sufficient for Dac function since we were unable to stably express it by itself. Instead, domains flanking DD1 are required to stabilize the protein, perhaps by assisting in its folding. Since the first 30 aa of Dac are left intact in ΔN, this appears to be sufficient to stabilize DD1. Since these 30 aa are not deleted in any of the stably expressed constructs, we cannot exclude the possibility that they may have an essential function. While N-DD1 is stably expressed, it is not sufficient for rescue. In contrast, N-DD1-M is both stable and capable of rescue, indicating that some sequence is needed C-terminal to DD1 for it to function properly. N-DD1-DD2 and N-DD1-M constructs rescue with similar efficiency suggesting that enabling rescue by DD1 may not require any specific sequence at its C-terminus.

An important advance in understanding DD1 function came with the resolution of the human DD1 crystal structure. This study determined that, although not predicted by its primary sequence, DD1 forms a helix-turn-helix motif similar to the winged helix family of DNA binding proteins and can bind DNA (Kim et al., 2002). Furthermore, other

studies have shown that mouse Dach1 can bind both to chromatin and, with lesser affinity, to naked DNA. The chromatin binding region of Dach1 was mapped to DD1 through deletion analysis (Ikeda et al., 2002). However, it is not yet known whether DD1 binds to a specific DNA sequence or to a higher order DNA structure.

In addition to its DNA binding ability, DD1 has a transactivator function as well. In yeast two-hybrid studies, expressing either full-length Dac or an N-terminal portion containing DD1 as prey (attached to the GAL4 DNA binding domain) results in activation of transcription, whereas expressing the N-terminal domain without DD1 does not (Chen et al., 1997). Thus, DD1 can bind DNA, regulate transcription, and perform the essential functions of Dac, most likely without the requirement of any other specific portion of the protein.

It is possible that DD1 can regulate transcription in a context-dependent manner. Specifically, DD1 from mouse Dach1 or human DACH1 can bind the corepressor proteins N-CoR and Histone deacetylase (HDAC) (Li et al., 2002; Wu et al., 2003). In the retina and pituitary gland, mouse Dach1 cooperates with Six6 and a corepressor complex to inhibit transcription of the cyclin-dependent kinase inhibitor *p27Kip1* (Li et al., 2002). In addition, cell culture studies revealed a role for human DACH1 as a repressor of TGF-β signaling (Wu et al., 2003). In contrast, synergistic transactivation among mouse Six5, Eya3, and Dach1 is dependent on the general transcriptional activator protein CBP (CREB binding protein) (Ikeda et al., 2002). Furthermore, the phosphatase function of Eya is important in switching Six1 and Dach1/2 from transcriptional repressors to activators in a murine myoblast cell culture system (Li et al., 2003).

Whether there are functional similarities between the Dach family and Ski/Sno is still an open question. Both factors can serve as corepressors and coactivators of transcription (Liu et al., 2001). Both factors bind the same domain of N-CoR through their N-terminal domains and recruit an HDAC complex to repress transcription (Li et al., 2002; Nomura et al., 1999). In cell culture, both Dach1/2 and Ski repress TGF-β signaling through Smad4 binding, but they use different domains to bind Smad4 (Wu et al., 2002, 2003). Dach1 DD1 and the N-terminal domain of Ski show 28% identity over an 83 aa stretch (Hammond et al., 1998). The conserved residues correspond largely to nonpolar amino acids that form the structural core of the domain and they may share the same tertiary structure (Kim et al., 2002). Although DD1 is capable of binding DNA, purified Ski has not been shown to do so thus far (Nagase et al., 1990). It may be that, the rest of the Ski protein may mask DNA binding activity of the N-terminal domain in Ski that is similar to DD1.

DD2 increases the efficiency with which DD1 functions

DD2 is a highly conserved domain predicted to form an α-helical structure. We have shown that *dac* mutants encoding proteins truncated before or within DD2 display moderate phenotypes in the eyes and legs. In addition, a missense mutation in DD2 causes a weak *dac* phenotype. Thus, our analysis of preexisting *dac* mutations suggests that DD2 must perform some function in Dac. In contrast, our rescue assay results indicate that DD2 is dispensable since multiple constructs lacking DD2 can fully rescue all *dac* phenotypes. This apparent discrepancy can be resolved if we consider a model where DD1 performs the critical function of Dac while DD2 facilitates DD1 function. Such a function would be masked in a rescue assay where the GAL4-UAS system results in elevated protein levels that can compensate for the lack of DD2. However, analysis of point mutants has revealed the consequences of altered Dac protein expressed at normal levels. Since point mutations specific to DD1 or DD2 both cause hypomorphic phenotypes, it would have been difficult to prioritize the function of these domains by mutant analysis alone. Instead, by using a GAL4-UAS rescue system in combination with analysis of preexisting mutations, we have been able to assign the critical function of Dac to DD1 and propose that DD2 serves to facilitate DD1.

One immediate question that comes from this model is how DD2 executes its function. We know from previous studies that DD2 interacts with a C-terminal conserved portion of Eya (ECD) in a yeast two-hybrid assay (Chen et al., 1997). Similarly, a partial cDNA encoding just DD2 was isolated in a yeast two-hybrid screen designed to identify proteins that interact with Eya (Bui et al., 2000). In the same study, a DD2-interacting domain in Eya was refined to a smaller region within ECD called EF1 (Bui et al., 2000). Direct physical interaction between Dac and Eya has also been shown by in vitro assays where GST-ECD pulled down full-length Dac and GST-DD2 pulled down full-length Eya (Chen et al., 1997). This physical interaction is conserved across species since chick Dach2 and Eya2 also bind to each other in GST pull-down assays (Heanue et al., 1999). These results suggest a very attractive model where DD2 facilitates Dac function through its physical interaction with Eya, which may stabilize the RD protein complex on DNA or provide an additional transactivation function. However, using an ectopic eye induction assay, we have shown that DD2 is not required for genetic synergy between Eya and Dac. Although ΔDD2, ΔNLS2, or N-DD1-M is not sufficient to induce ectopic eye formation by themselves, they do synergize with a weak *UAS-Eya* allele to induce large ectopic eye patches ventral to the antenna with high penetrance (Fig. 5). Since synergy experiments are conducted in a wild-type *dac* background, we cannot rule out the possibility that Eya-mediated induction of endogenous Dac might contribute to ectopic eye formation. However, misexpression of any Dac construct alone is not sufficient to induce endogenous Dac expression (data not shown). Although Eya is capable of inducing low levels of endogenous Dac, it cannot induce ectopic eyes of the same size and penetrance as any combination of Dac/Eya. Therefore, we conclude that Dac and Eya synergize in the absence of DD2.

Furthermore, an Eya mutation within EF1 that abrogates the interaction with DD2 in a yeast two-hybrid assay is still able to synergize with Dac (Bui et al., 2000). Moreover, no interaction between Eya and Dac was detected in a *Drosophila* S2 cell two-hybrid system (Silver et al., 2003). Even if an Eya–Dac interaction occurs in vivo, it is unlikely to be the only mechanism by which DD2 assists DD1. In addition, an Eya–Dac interaction may be significant only in the context of eye development since Eya is not present in most tissues where Dac is expressed. Since DD2 truncation results in a mutant phenotype with eyes and legs equally affected, DD2 must have a more general role than just binding Eya.

Since DD2 is predicted to form an α-helical structure with a strong tendency to form a coiled-coil, an alternate model for DD2 function is through formation of a coiled-coil homodimer, which may in turn stabilize DD1 on DNA or amplify its transactivator function. In fact, c-Ski protein, which shares similarity with DD1, also contains a C-terminal α-helical coiled-coil domain. Although DD2 and the Ski C-terminal domain are divergent in their primary sequence, they share significant similarities in their predicted secondary structure (Hammond et al., 1998). In addition to homodimerizing, the C-terminal domain of Ski can also heterodimerize with the Ski-related protein SnoN with high affinity (Heyman and Stavnezer, 1994b; Nagase et al., 1993; Zheng et al., 1997a). It is interesting to note that v-Ski, the viral oncogene that is thought to be a deleted form of c-Ski, does not contain the C-terminal α-helical domain. v-Ski is able to induce transformation and promote muscle differentiation in embryonic quail fibroblasts. However, the cellular counterpart c-Ski is much more potent than v-Ski in its transformation and differentiation capabilities, suggesting that the N-terminal domain is sufficient for both functions while α-helical domain is required for increased efficiency (Zheng et al., 1997b). Thus, the structural similarities between Ski and Dac may extend to functional conservation as well, with the N-terminal domain providing the critical function while the C-terminal domain assists it to function at full capacity. Although we have not observed a homotypic interaction for Dac in vitro, Dac may homodimerize in vivo. Alternatively, Dac may interact via DD2 with other unidentified proteins to mediate its function.

Subcellular localization of Dac is primarily dependent on DD1

We have shown that DD1, DD2, and a basic NLS sequence in the middle domain are each sufficient to translocate 3xGFP or an N-terminal domain of Dac to the nucleus. There are no recognizable NLS sequences in DD1 and a 7-aa stretch at the C-terminus of DD1 most similar to an NLS was not sufficient to direct 3xGFP to the nucleus. Even though there is a predicted bipartite NLS that resides in DD2 and is conserved across species, this signal is neither sufficient nor necessary for nuclear localization of Dac in salivary gland cells and is not required in any other tissues in which Dac is normally expressed. Therefore, DD1 and DD2 may target Dac to the nucleus through either a novel signal or protein–protein interactions with other nuclear factors. We argue that DD1 is the most important domain for nuclear localization since deletion of DD1 compromises the subcellular localization of Dac, whereas deletion of the middle domain, DD2, or both does not cause any detectable mislocalization. Involvement of DD1 in nuclear localization raises the possibility that the inability of ΔDD1 to rescue *dac* phenotypes is due to improper localization. However, we find approximately 50% of ΔDD1 protein in the nucleus and missense mutations in DD1 display severe phenotypes even though their protein products are nuclear, making this possibility unlikely.

Since both the N-terminal domain and 3xGFP protein are uniformly distributed in the cell in our assays, and DD1 and DD2 are capable of binding DNA or proteins, respectively, another possibility could be that DD1 and DD2 are not directly involved in nuclear localization. Instead, the nuclear localization observed with N-DD1, N-DD2, and 3xGFP-DD1 may be due to retention of these proteins in the nucleus following simple diffusion. This argument is valid for DD2 since it is not required for proper subcellular localization of Dac. However, DD1 is directly involved since it is both necessary and sufficient for nuclear localization.

A mammalian cell culture study suggests that Dach1 moves between the nucleus and the perinuclear zone in a cell cycle-dependent manner with the help of the mouse ubiquitin-conjugating enzyme Ubc9 (Machon et al., 2000). However, we do not detect a similar movement of Dac between the nucleus and cytoplasm in *Drosophila*: Dac staining in imaginal discs and Kenyon cells in the brain is exclusively nuclear to the best of our detection abilities. In addition, we examined the possibility of a genetic interaction between loss-of-function mutations in a *Drosophila* homolog of *Ubc9* (*lesswright*) and *dac* but none was observed (data not shown). Ubc9 was shown to bind the C-terminal half of Dach1 but not DD2 in yeast two-hybrid experiments (Machon et al., 2000). Thus, it is possible that Ubc9 binds Dach1 through the nonconserved middle portion of the protein, thereby providing a mode of regulation of Dach that may be specific to vertebrates.

Acknowledgments

We would like to thank Iain Dawson, Kevin Moses, Mitzi Kuroda, Francesca Pignoni, and Larry Zipursky for providing fly stocks; Cornelius Boerkoel and George Halder for use of their Leica stereomicroscopes; Anh Dang for sequencing services; Kartik Pappu for critical reading of the manuscript; and Richard Davis for the brain dissection protocol. We thank MD Anderson SEM core

(cancer center core grant CA 16672) for their work. This work was supported by funds awarded to G.M. from the National Eye Institute (R01 EY11232-01), the Baylor Mental Retardation Research Center (P30 HD24064), and the Retina Research Foundation.

References

Backman, M., Machon, O., Van Den Bout, C.J., Krauss, S., 2003. Targeted disruption of mouse Dach1 results in postnatal lethality. Dev. Dyn. 226, 139–144.

Bertuccioli, C., Fasano, L., Jun, S., Wang, S., Sheng, G., Desplan, C., 1996. In vivo requirement for the paired domain and homeodomain of the paired segmentation gene product. Development 122, 2673–2685.

Blackman, R.K., Sanicola, M., Raftery, L.A., Gillevet, T., Gelbart, W.M., 1991. An extensive 3′ *cis*-regulatory region directs the imaginal disk expression of decapentaplegic, a member of the TGF-beta family in *Drosophila*. Development 111, 657–666.

Bonini, N.M., Leiserson, W.M., Benzer, S., 1993. The eyes absent gene: genetic control of cell survival and differentiation in the developing *Drosophila* eye. Cell 72, 379–395.

Bonini, N.M., Bui, Q.T., Gray-Board, G.L., Warrick, J.M., 1997. The *Drosophila* eyes absent gene directs ectopic eye formation in a pathway conserved between flies and vertebrates. Development 124, 4819–4826.

Brand, A.H., Perrimon, N., 1993. Targeted gene expression as a means of altering cell fates and generating dominant phenotypes. Development 118, 401–415.

Bui, Q.T., Zimmerman, J.E., Liu, H., Bonini, N.M., 2000. Molecular analysis of *Drosophila* eyes absent mutants reveals features of the conserved Eya domain. Genetics 155, 709–720.

Caubit, X., Thangarajah, R., Theil, T., Wirth, J., Nothwang, H.G., Ruther, U., Krauss, S., 1999. Mouse Dac, a novel nuclear factor with homology to *Drosophila* dachshund shows a dynamic expression in the neural crest, the eye, the neocortex, and the limb bud. Dev. Dyn. 214, 66–80.

Chen, R., Amoui, M., Zhang, Z.H., Mardon, G., 1997. Dachshund and eyes absent proteins form a complex and function synergistically to induce ectopic eye development in *Drosophila*. Cell 91, 893–903.

Chen, R., Halder, G., Zhang, Z., Mardon, G., 1999. Signaling by the TGF-ß homolog decapentaplegic functions reiteratively within the network of genes controlling retinal cell fate determination in *Drosophila*. Development 126, 935–943.

Cheyette, B.N., Green, P.J., Martin, K., Garren, H., Hartenstein, V., Zipursky, S.L., 1994. The *Drosophila* sine oculis locus encodes a homeodomain-containing protein required for the development of the entire visual system. Neuron 12, 977–996.

Davis, R.J., Shen, W., Heanue, T.A., Mardon, G., 1999. Mouse Dach, a homologue of *Drosophila* dachshund, is expressed in the developing retina, brain and limbs. Dev. Genes Evol. 209, 526–536.

Davis, R.J., Shen, W., Sandler, Y.I., Amoui, M., Purcell, P., Maas, R., Ou, C.N., Vogel, H., Beaudet, A.L., Mardon, G., 2001a. Dach1 mutant mice bear no gross abnormalities in eye, limb, and brain development and exhibit postnatal lethality. Mol. Cell. Biol. 21, 1484–1490.

Davis, R.J., Shen, W., Sandler, Y.I., Heanue, T.A., Mardon, G., 2001b. Characterization of mouse Dach2, a homologue of *Drosophila* dachshund. Mech. Dev. 102, 169–179.

Davis, R.J., Tavsanli, B.C., Dittrich, C., Walldorf, U., Mardon, G., 2003. *Drosophila* retinal homeobox (drx) is not required for establishment of the visual system, but is required for brain and clypeus development. Dev. Biol. 259, 272–287.

Dong, P.D., Dicks, J.S., Panganiban, G., 2002. Distal-less and homothorax regulate multiple targets to pattern the *Drosophila* antenna. Development 129, 1967–1974.

Gorlich, D., Kutay, U., 1999. Transport between the cell nucleus and the cytoplasm. Annu. Rev. Cell Dev. Biol. 15, 607–660.

Halder, G., Callaerts, P., Gehring, W.J., 1995. Induction of ectopic eyes by targeted expression of the eyeless gene in *Drosophila*. Science 267, 1788–1792.

Halder, G., Callaerts, P., Flister, S., Walldorf, U., Kloter, U., Gehring, W.J., 1998. Eyeless initiates the expression of both sine oculis and eyes absent during *Drosophila* compound eye development. Development 125, 2181–2191.

Hammond, K.L., Hanson, I.M., Brown, A.G., Lettice, L.A., Hill, R.E., 1998. Mammalian and *Drosophila* dachshund genes are related to the Ski proto-oncogene and are expressed in eye and limb. Mech. Dev. 74, 121–131.

Hanson, I.M., 2001. Mammalian homologues of the *Drosophila* eye specification genes. Semin. Cell Dev. Biol. 12, 475–484.

Heanue, T.A., Reshef, R., Davis, R.J., Mardon, G., Oliver, G., Tomarev, S., Lassar, A.B., Tabin, C.J., 1999. Synergistic regulation of vertebrate muscle development by Dach2, Eya2, and Six1, homologs of genes required for *Drosophila* eye formation. Genes Dev. 13, 3231–3243.

Heyman, H.C., Stavnezer, E., 1994a. A *carboxyl*-terminal region of the ski oncoprotein mediates homodimerization as well as heterodimerization with the related protein SnoN. J. Biol. Chem. 269, 26996–27003.

Heyman, H.C., Stavnezer, E., 1994b. A *carboxyl*-terminal region of the ski oncoprotein mediates homodimerization as well as heterodimerization with the related protein SnoN. J. Biol. Chem. 269, 26996–27003.

Hsiao, F.C., Williams, A., Davies, E.L., Rebay, I., 2001. Eyes absent mediates cross-talk between retinal determination genes and the receptor tyrosine kinase signaling pathway. Dev. Cell 1, 51–61.

Ikeda, K., Watanabe, Y., Ohto, H., Kawakami, K., 2002. Molecular interaction and synergistic activation of a promoter by Six, Eya, and Dach proteins mediated through CREB binding protein. Mol. Cell. Biol. 22, 6759–6766.

Keisman, E.L., Baker, B.S., 2001. The *Drosophila* sex determination hierarchy modulates wingless and decapentaplegic signaling to deploy dachshund sex-specifically in the genital imaginal disc. Development 128, 1643–1656.

Kim, S.S., Zhang, R.G., Braunstein, S.E., Joachimiak, A., Cvekl, A., Hegde, R.S., 2002. Structure of the retinal determination protein Dachshund reveals a DNA binding motif. Structure (Camb.) 10, 787–795.

Kimmel, B.E., Heberlein, U., Rubin, G.M., 1990. The homeo domain protein rough is expressed in a subset of cells in the developing *Drosophila* eye where it can specify photoreceptor cell subtype. Genes Dev. 4, 712–727.

Kurusu, M., Nagao, T., Walldorf, U., Flister, S., Gehring, W.J., Furukubo-Tokunaga, K., 2000. Genetic control of development of the mushroom bodies, the associative learning centers in the *Drosophila* brain, by the eyeless, twin of eyeless, and dachshund genes. Proc. Natl. Acad. Sci. U. S. A. 97, 2140–2144.

Li, X., Perissi, V., Liu, F., Rose, D.W., Rosenfeld, M.G., 2002. Tissue-specific regulation of retinal and pituitary precursor cell proliferation. Science 297, 1180–1183.

Li, X., Oghi, K.A., Zhang, J., Krones, A., Bush, K.T., Glass, C.K., Nigam, S.K., Aggarwal, A.K., Maas, R., Rose, D.W., Rosenfeld, M.G., 2003. Eya protein phosphatase activity regulates Six1-Dach-Eya transcriptional effects in mammalian organogenesis. Nature 426, 247–254.

Liu, X., Sun, Y., Weinberg, R.A., Lodish, H.F., 2001. Ski/Sno and TGF-beta signaling. Cytokine Growth Factor Rev. 12, 1–8.

Machon, O., Backman, M., Julin, K., Krauss, S., 2000. Yeast two-hybrid system identifies the ubiquitin-conjugating enzyme mUbc9 as a potential partner of mouse Dac. Mech. Dev. 97, 3–12.

Mardon, G., Solomon, N.M., Rubin, G.M., 1994. Dachshund encodes a nuclear protein required for normal eye and leg development in *Drosophila*. Development 120, 3473–3486.

Martini, S.R., Roman, G., Meuser, S., Mardon, G., Davis, R.L., 2000. The retinal determination gene, dachshund, is required for mushroom body cell differentiation. Development 127, 2663–2672.

Moses, K., Rubin, G.M., 1991. Glass encodes a site-specific DNA-binding protein that is regulated in response to positional signals in the developing *Drosophila* eye. Genes Dev. 5, 583–593.

Nagase, T., Mizuguchi, G., Nomura, N., Ishizaki, R., Ueno, Y., Ishii, S., 1990. Requirement of protein co-factor for the DNA-binding function of the human ski proto-oncogene product. Nucleic Acids Res. 18, 337–343.

Nagase, T., Nomura, N., Ishii, S., 1993. Complex formation between proteins encoded by the ski gene family. J. Biol. Chem. 268, 13710–13716.

Nomura, T., Khan, M.M., Kaul, S.C., Dong, H.D., Wadhwa, R., Colmenares, C., Kohno, I., Ishii, S., 1999. Ski is a component of the histone deacetylase complex required for transcriptional repression by Mad and thyroid hormone receptor. Genes Dev. 13, 412–423.

Noveen, A., Daniel, A., Hartenstein, V., 2000. Early development of the *Drosophila* mushroom body: the roles of eyeless and dachshund. Development 127, 3475–3488.

Pignoni, F., Hu, B., Zavitz, K.H., Xiao, J., Garrity, P.A., Zipursky, S.L., 1997. The eye-specification proteins So and Eya form a complex and regulate multiple steps in *Drosophila* eye development. Cell 91, 881–891.

Punzo, C., Kurata, S., Gehring, W.J., 2001. The eyeless homeodomain is dispensable for eye development in *Drosophila*. Genes Dev. 15, 1716–1723.

Quiring, R., Walldorf, U., Kloter, U., Gehring, W.J., 1994. Homology of the eyeless gene of *Drosophila* to the Small eye gene in mice and aniridia in humans [see comments]. Science 265, 785–789.

Rayapureddi, J.P., Kattamuri, C., Steinmetz, B.D., Frankfort, B.J., Ostrin, E.J., Mardon, G., Hegde, R.S., 2003. Eyes absent represents a class of protein tyrosine phosphatases. Nature 426, 295–298.

Robinow, S., White, K., 1991. Characterization and spatial distribution of the ELAV protein during *Drosophila* melanogaster development. J. Neurobiol. 22, 443–461.

Rubin, G.M., Spradling, A.C., 1982. Genetic transformation of *Drosophila* with transposable element vectors. Science 218, 348–353.

Sepp, K.J., Auld, V.J., 1999. Conversion of lacZ enhancer trap lines to GAL4 lines using targeted transposition in *Drosophila* melanogaster. Genetics 151, 1093–1101.

Shen, W., Mardon, G., 1997. Ectopic eye development in *Drosophila* induced by directed dachshund expression. Development 124, 45–52.

Silver, S.J., Davies, E.L., Doyon, L., Rebay, I., 2003. Functional dissection of eyes absent reveals new modes of regulation within the retinal determination gene network. Mol. Cell. Biol. 23, 5989–5999.

Spradling, A.C., Rubin, G.M., 1982. Transposition of cloned P elements into *Drosophila* germ line chromosomes. Science 218, 341–347.

Staehling-Hampton, K., Hoffmann, F.M., 1994. Ectopic decapentaplegic in the *Drosophila* midgut alters the expression of five homeotic genes, dpp, and wingless, causing specific morphological defects. Dev. Biol. 164, 502–512.

Tomlinson, A., Ready, D.F., 1987. Cell fate in the *Drosophila* ommatidium. Dev. Biol. 123, 264–275.

Tootle, T.L., Silver, S.J., Davies, E.L., Newman, V., Latek, R.R., Mills I.A., Selengut, J.D., Parlikar, B.E., Rebay, I., 2003. The transcription factor eyes absent is a protein tyrosine phosphatase. Nature 426, 299–302.

Wu, J.W., Krawitz, A.R., Chai, J., Li, W., Zhang, F., Luo, K., Shi, Y., 2002. Structural mechanism of Smad4 recognition by the nuclear oncoprotein Ski: insights on Ski-mediated repression of TGF-beta signaling. Cell 111, 357–367.

Wu, K., Yang, Y., Wang, C., Davoli, M.A., D'Amico, M., Li, A., Cveklova, K., Kozmik, Z., Lisanti, M.P., Russell, R.G., Cvekl, A., Pestell, R.G., 2003. DACH1 inhibits TGF-beta signaling through binding Smad4. J. Biol. Chem. 278, 51673–51684.

Zheng, G., Blumenthal, K.M., Ji, Y., Shardy, D.L., Cohen, S.B., Stavnezer, E., 1997a. High affinity dimerization by Ski involves parallel pairing of a novel bipartite alpha-helical domain. J. Biol. Chem. 272, 31855–31864.

Zheng, G., Teumer, J., Colmenares, C., Richmond, C., Stavnezer, E., 1997b. Identification of a core functional and structural domain of the v-Ski oncoprotein responsible for both transformation and myogenesis. Oncogene 15, 459–471.